

Nature of the pressure-induced magnetic phase transition in the itinerant-electron antiferromagnet YMn_2 : A microscopic view

Andreas Block, Mohsen M. Abd-Elmeguid,* and Hans Micklitz*

Experimentalphysik IV, Ruhr-Universität Bochum, 44780 Bochum, Federal Republic of Germany

(Received 4 January 1994)

The ^{119}Sn high-pressure Mössbauer-effect technique on 0.5 at. % ^{119}Sn -doped YMn_2 has been used to investigate, on a microscopic level, the nature of the pressure-induced magnetic-to-nonmagnetic phase transition in the itinerant-electron antiferromagnet YMn_2 . We find, in contrast to the temperature-induced first-order magnetic phase transition at T_N and at ambient pressure, a strong but continuous reduction of the ordered Mn local magnetic moment in the range $0 \leq p < 0.3$ GPa, which reveals a pressure-induced second-order phase transition. In the same pressure range, we observe a change of the nature of the spin fluctuations from transversal ($0 \leq p < 0.3$ GPa) to longitudinal at higher pressures. We further show evidence for short-range magnetic order in the pressure-induced nonmagnetic state ($0.3 \leq p \leq 4$ GPa).

The rare-earth (R) Laves-phase intermetallic compounds RMn_2 show a variety of magnetic and structural properties depending on R .¹⁻³ Among these YMn_2 ($C15$ -type structure) reveals various interesting temperature-induced magnetic and structural phenomena which recently have been the subject of a large number of experimental⁴⁻⁸ and theoretical⁹ efforts. The prime interest in YMn_2 is connected with the fact that this compound is considered as a unique system which exhibits *both* localized and weak itinerant magnetic properties and thereby allows one to investigate the mechanism of moment formation in a magnetic system: YMn_2 develops an antiferromagnetic (AF) order below $T_N \approx 100$ K,^{4,10,11} where the Mn moments are predominantly localized ($\mu_{\text{Mn}} = 2.7\mu_B$).¹² However, at $T = T_N$ the Mn moments suddenly collapse, suggesting a transition from local moment to weak itinerant magnetism. This magnetic phase transition is of first order, where the collapse of the Mn moments above T_N is accompanied by a giant volume decrease of the unit cell ($\Delta V/V \approx 5\%$).¹ The magnetic properties above T_N are characterized by strong longitudinal spin fluctuations (SF).¹²

The above-mentioned strong coupling between magnetism and volume in YMn_2 (large magnetovolume effect) very recently has stimulated many experimental groups to investigate the effect of pressure on the magnetic properties of YMn_2 .¹³⁻¹⁵ The main result of all these *macroscopic* high pressure experiments (electrical resistivity,¹³ specific heat¹⁴ and elastic neutron scattering¹⁵) is the observation of a magnetic-to-nonmagnetic phase transition at pressures between 0.2 and 0.3 GPa depending on the sample. Evidence for the enhancement of the spin fluctuations (SF) at the magnetic \rightarrow nonmagnetic phase transition is reported from the high pressure specific heat data.¹⁴ However, several crucial questions are raised by these experimental results: (1) What is the mechanism of the disappearance of the localized Mn moment under high pressure, (2) is there a corresponding pressure-induced change of the nature of the spin fluctuations at the magnetic phase transition, and (3) what is the nature of the pressure-induced

nonmagnetic state?

In order to provide a microscopic insight into these questions, we have performed ^{119}Sn high pressure Mössbauer effect (ME) experiments up to 4 GPa on YMn_2 samples doped with 0.5 at. % ^{119}Sn . Using the ME technique, the stability of the Mn local magnetic moment can be measured via the pressure-induced variation of the average transferred magnetic hyperfine (HF) field, \bar{B}_{THF} at the ^{119}Sn nucleus [$\bar{B}_{\text{THF}}(p) \propto \mu_{\text{Mn}}(p)$]. In addition, this technique allows the determination of the pressure dependence of T_N by measuring the temperature dependence of \bar{B}_{THF} at each value of the applied pressure.

The sample of $\text{Y}(\text{Mn}_{0.995}\text{Sn}_{0.005})_2$ was prepared by induction melting on a water-cooled Cu finger in a pure argon atmosphere. Stoichiometric amounts of ^{119}Sn and Mn were premelted in order to obtain a homogeneous distribution of ^{119}Sn on the Mn sites in YMn_2 . No further annealing of the sample was done in order to avoid possible site changing of ^{119}Sn atoms from Mn to Y sites. Details of the preparation procedure are described elsewhere.¹⁶ Powder x-ray diffraction patterns show the pure cubic ($C15$) Laves-phase structure of YMn_2 . We find neither traces of the Y_6Mn_{23} phase nor of Y metal. The value of T_N has been determined from the dc susceptibility ($T_N \approx 70$ K). This value is smaller than the value of T_N for YMn_2 , possibly due to local disorder in the nonannealed sample. All other macroscopic properties of our doped YMn_2 sample,¹⁶ on the other hand, are in good agreement with those known for YMn_2 :¹ from the temperature dependence of the x-ray diffraction patterns we obtain the *same* value of the volume change ($\Delta V/V \approx 5\%$) at T_N . We also obtain for our sample the *same* value of the thermal expansion coefficient ($\alpha \approx 50 \times 10^{-6} \text{K}^{-1}$, $T > T_N$) known for YMn_2 (Ref. 5). ^{119}Sn high pressure ME experiments up to 4 GPa and at different temperatures from 300 to 1.6 K were performed using a Chester-Jones type high-pressure setup as describe elsewhere.¹⁷ A $\text{Ca } ^{119}\text{SnO}_3$ Mössbauer source was used (5 mCi, 4 mm active diameter).

The ^{119}Sn ME spectra of YMn_2 as a function of tem-

perature and of pressure are shown in Figs. 1, 2(a), and 2(b), respectively. All ME spectra were fitted using a modified histogram method as described in Ref. 18 which allows one to obtain the values of the average transferred HF field \bar{B}_{THF} and its distribution $P(B_{\text{THF}})$, see Fig. 3, which reflects the distribution of Mn local magnetic moments around the ^{119}Sn probe. Figure 1 shows some selected ME spectra at different temperatures collected upon cooling and heating the sample at ambient pressure. We obtain in the paramagnetic state ($T > T_N$) a linewidth of 1 mm/s which we have taken as a constant in the analysis of the ME spectra in the magnetic state. The analysis of the ME at 4.2 K and at $p = 0$ GPa shows that the HF field distribution does not contain any nonmagnetic component. This proves that the ^{119}Sn probe occupies only Mn sites, because one expects no transferred HF field if Sn would occupy Y sites in the C15 structure. Within the experimental error we do find at the phase transitions neither temperature-induced nor pressure-induced change of the isomer shift [$S = 1.75(4)$ mm/s]. Figure 2(a) displays the pressure dependence of the ME spectra collected at 4.2 K (0, 0.2, and 0.3 GPa) or at 1.6 K (0.8 and 4.0 GPa), whereas Fig. 2(b) shows the temperature dependence of the ME spectra at $P = 0.3$ GPa. The pressure dependence of \bar{B}_{THF} and of T_N as obtained from the analysis of the corresponding ME spectra is plotted in Fig. 3. Here, we find a sharp, but discontinuous decrease of \bar{B}_{THF} and in particular of T_N with increasing pressure, which indicates a pressure-induced magnetic phase transition at a critical pressure $p_c = 0.3$ GPa from the AF state to another magnetic state with much lower values of $T_N = 15$ K and $\mu_{\text{Mn}} < 0.5\mu_B$ (obtained at $p \geq 1.0$ GPa; see Fig. 3). \bar{B}_{THF} and T_N approach zero by further increasing the pressure $0.3 \leq p \leq 4.0$ GPa. The relative decrease of \bar{B}_{THF} with pressure for $0 \leq p \leq 0.27$ GPa is in good agreement with the relative decrease of μ_{Mn} with pressure (Fig. 3) as obtained from very recent elastic neutron scattering measurements of YMn_2 under high pressure.¹⁵ Also the rate of decrease of T_N with p , $dT_N/dp = -110$ K GPa⁻¹ is comparable with that obtained from previous

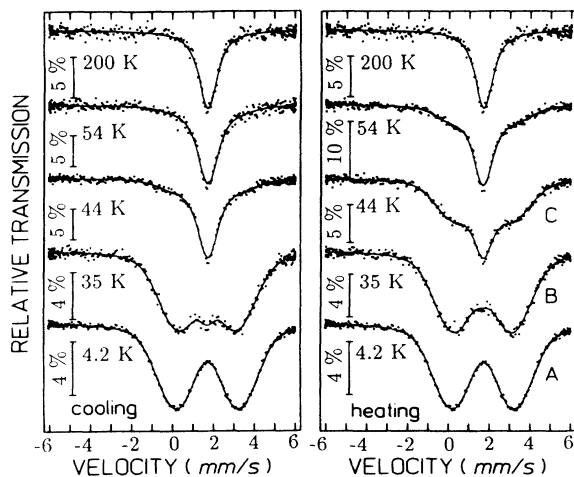


FIG. 1. Temperature dependence of the ^{119}Sn Mössbauer spectra at ambient pressure upon heating and cooling of YMn_2 sample doped with 0.5 at. % ^{119}Sn .

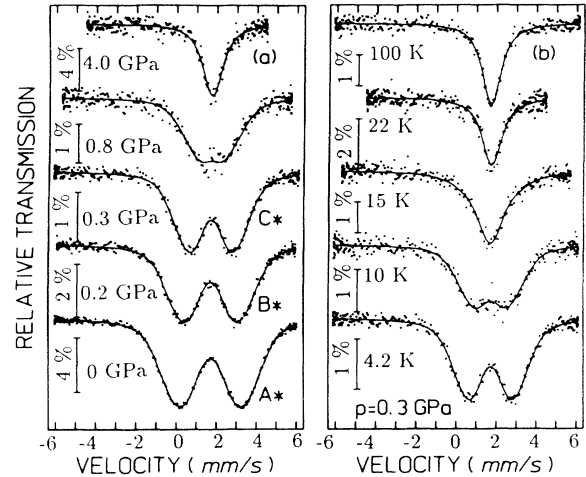


FIG. 2. (a) Pressure dependence of the ^{119}Sn Mössbauer spectra of YMn_2 sample doped with 0.5 at. % ^{119}Sn collected at 4.2 K ($p = 0, 0.2$, and 0.3 GPa) and at 1.6 K ($p = 0.8$ and 4.0 GPa). (b) Temperature dependence of the ^{119}Sn Mössbauer spectra of the same sample at $p = 0.3$ GPa.

high pressure measurements.^{7,8}

In the following we discuss the first-order magnetic phase transition in YMn_2 which occurs at ambient pressure.⁴ As evident from Fig. 1, the temperature dependence of the ME spectra at ambient pressure displays the features that are expected for a first-order magnetic phase transition: one observes upon cooling (or heating) in Fig. 1 the coexistence of a magnetic and a nonmagnetic (single line) component at temperatures near T_N . This is best seen from the corresponding temperature variation of the HF field distribution $P(B_{\text{THF}})$ shown in Fig. 4(a). One observes upon heating the evolution of the nonmagnetic component at the expense of the magnetic one, while no shift between the two components occurs. In addition, we find a thermal hysteresis as expected for a first-order transition in YMn_2 . This is clearly seen in Fig. 1 by comparing the ME spectra for cooling and heating at the same temperature (e.g., at $T = 35$ K).

In contrast to the temperature-induced, first-order

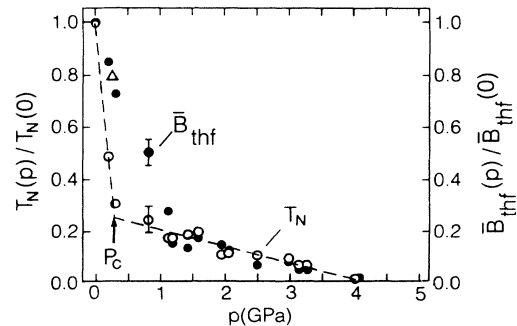


FIG. 3. Pressure dependence of the relative changes of T_N , $T_N(p)/T_N(0)$, and of \bar{B}_{THF} , $\bar{B}_{\text{THF}}(p)/\bar{B}_{\text{THF}}(0)$, for ^{119}Sn doped YMn_2 as deduced from the analysis of the corresponding ^{119}Sn ME spectra. The symbol Δ denotes the relative decrease of μ_{Mn} at $p = 0.27$ GPa as obtained from elastic neutron scattering (Ref. 15). Lines through data points of T_N are only a guide to the eye.

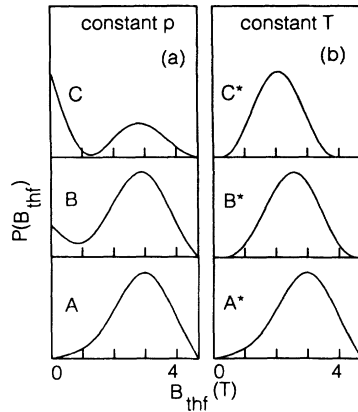


FIG. 4. (a) Temperature variation of the HF field distribution $P(B_{\text{THF}})$ at ambient pressure for ^{119}Sn doped YMn_2 sample as obtained from the analysis of the corresponding ^{119}Sn ME spectra. Symbols A, B, and C denote the HF field distributions of the ME spectra A, B, and C in Fig. 1 (heating). (b) Pressure variation of $P(B_{\text{THF}})$ at $T = 4.2$ K for the same YMn_2 sample as obtained from the analysis of the corresponding ^{119}Sn ME spectra. Symbols A*, B*, and C* denote the HF field distributions of the ME spectra A*, B*, and C* in Fig. 2(a).

magnetic phase transition at T_N and at ambient pressure, we find a *continuous* reduction of the Mn local magnetic moment in the range $0 \leq p \leq 0.3$ GPa [see Fig. 2(a)], which reveals a pressure-induced *second-order* phase transition. This is evident from the *gradual* shift of the maximum in the HF field distribution from the AF component towards the nonmagnetic component [Fig. 4(b)]. Further support for a pressure-induced magnetic phase transition of second order is the absence of the temperature-induced hysteresis at $p = 0.3$ GPa [Fig. 2(b)] as compared with that obtained at $p = 0$ GPa (Fig. 1). In this respect, we want to emphasize that our finding of a second-order phase transition of the ordered Mn moments in YMn_2 contradicts the conclusion drawn from very recent high pressure elastic neutron scattering, namely, of an inhomogeneous decrease of μ_{Mn} with pressure $0 \leq p \leq 0.27$ GPa.¹⁵

Next, we want to discuss the role of spin fluctuations with respect to the pressure-induced magnetic phase transition in YMn_2 at p_c . In order to do this, we have plotted in Fig. 5 the normalized values of \bar{B}_{THF} , $b = \bar{B}_{\text{THF}}(p, T) / \bar{B}_{\text{THF}}(p = 0, T = 4.2 \text{ K})$, which correspond to $\mu_{\text{Mn}}(p, T) / \mu_{\text{Mn}}(p = 0, T = 4.2 \text{ K})$ against the normalized temperature $[T / T_N(p = 0)]$ for various values of the pressure. The difference in the temperature dependence of μ_{Mn} between $p = 0$ and 0.2 GPa, on one hand, and $p = 0.3$ GPa, on the other hand, is clearly demonstrated in Fig. 5. A comparison of the temperature dependence of μ_{Mn} with the temperature dependence of the amplitude of the local spin fluctuations S_L^2 (Ref. 19) suggests that μ_{Mn} in YMn_2 under high pressure exhibits a change from mainly transversal SF typical for local moment behavior (first-order phase transition) for $p < p_c$ to longitudinal SF typical for weak itinerant magnetism ($p = p_c$). This finding is strongly supported by the following quantitative analysis: from

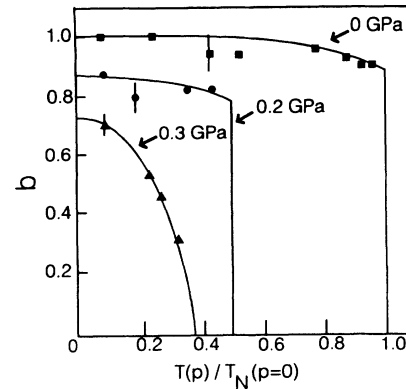


FIG. 5. Temperature dependence of the normalized transferred HF field, $b = \bar{B}_{\text{THF}}(p, T) / \bar{B}_{\text{THF}}(p = 0, T = 4.2 \text{ K})$, which has been determined from the corresponding HF field distributions taking only into account the magnetic component (see Fig. 4). Lines through data points are only a guide to the eye.

Fig. 3 one obtains for $p_c \leq p \leq 4$ GPa a value of $d \ln T_N / dp \approx d \ln \bar{B}_{\text{THF}} / dp$ as expected from the theory for very weak itinerant-electron ferromagnets.²⁰

Finally, we want to compare the pressure-induced magnetic phase transition in YMn_2 detected by ^{119}Sn ME spectroscopy as a microscopic tool with that measured by macroscopic high pressure methods.^{13–15}

As mentioned above, both the pressure-induced changes of μ_{Mn} and T_N obtained from Me ^{119}Sn high pressure technique are in agreement with those obtained from elastic neutron scattering¹⁵ and electrical resistivity,⁸ respectively. However, there is a difference between the high pressure ME results and those obtained from other (macroscopic) high pressure experiments: we observe at p_c a magnetic phase transition from the predominantly localized AF state to another magnetic state with a much lower Mn-magnetic moment $\leq 0.5 \mu_B$ instead of $2.7 \mu_B$ at ambient pressure which is suppressed to zero at 4 GPa (see Fig. 3). This observation appears to contradict with other high pressure experimental results, namely the observation of a magnetic-to-nonmagnetic phase transition at p_c . However, since high pressure results on YMn_2 as obtained from elastic neutron scattering¹⁵ and from low-temperature specific heat¹⁴ exclude any existence of long-range magnetic order above p_c , we attribute our observation of a “low-moment” magnetic state above p_c by ^{119}Sn ME spectroscopy to be due to a short-range magnetic order. This can be originated from freezing of the spin fluctuations which exhibit strong AF correlations in the neighborhood of the ^{119}Sn probe in YMn_2 . This conclusion is consistent with our finding that increasing pressure to p_c has the effect of enhancement of the longitudinal SF in YMn_2 (see Fig. 5).

In this connection, it is interesting to refer to recent studies of the effect of *chemical pressure* on the magnetic properties of YMn_2 .^{21,22} Here it is shown that doping of 3 at. % of Sc for Y in YMn_2 (i.e., $\text{Y}_{0.97}\text{Sc}_{0.03}\text{Mn}_2$) which reduces the volume by about 1% destroys the long-range AF order. In this “nonmagnetic” state one finds²¹ evidence for short-range AF correlations from inelastic neu-

tron scattering measurements on $Y_{0.97}Sc_{0.03}Mn_2$ as well as an enhancement of γ ($\gamma = 140 \text{ mJ/K}^2 \text{ mol}$) from measurements of specific heat at low temperatures.²² These results are consistent both with the enhancement of γ by external pressure,¹⁴ and with our observation of short-range magnetic order in the pressure-induced nonmagnetic state of YMn_2 .

In summary, we find in contrast to the temperature-induced first-order magnetic phase transition at T_N and at ambient pressure a continuous reduction of the Mn local magnetic moment in the range $0 \leq p < 0.3 \text{ GPa}$,

which reveals a pressure-induced second-order phase transition. In the same pressure range, we observe a change of the nature of the spin fluctuations from transversal SF ($0 \leq p < 0.3 \text{ GPa}$) to longitudinal SF at higher pressures ($p \geq 0.3 \text{ GPa}$). We further show evidence for short-range magnetic order in the pressure-induced nonmagnetic state ($0.3 \leq p < 4 \text{ GPa}$).

The authors would like to thank E. Holland-Moritz, D. Wagner, and K. Westerholt for helpful discussions. This work was supported by the Deutsche Forschungsgemeinschaft (SFB 166).

* Present address: II. Physikalisches Institut, Universität zu Köln, Zùlpicherstr. 77, 50937 Köln, Germany.

¹ Y. Nakamura, *J. Magn. Magn. Mater.* **31-34**, 829 (1983).

² K. Yoshimura, M. Shiga, and Y. Nakamura *J. Phys. Soc. Jpn.* **55**, 3585 (1986).

³ W. Hussen *et al.*, *J. Magn. Magn. Mater.* **84**, 281 (1990).

⁴ Y. Nakamura, M. Shiga, and S. Kawano, *Physica B* **120**, 212 (1983).

⁵ H. Wada *et al.*, *J. Magn. Magn. Mater.* **70**, 134 (1987).

⁶ L. Asch *et al.*, *Hyperfine Interact.* **64**, 435 (1990).

⁷ G. Oomi *et al.*, *J. Magn. Magn. Mater.* **70**, 137 (1987).

⁸ N. H. Kim-Ngan *et al.*, *Physica B* **179**, 231 (1992).

⁹ R. Ballou, C. Lacroix, and M. D. Nunez Regueiro, *Phys. Rev. Lett.* **66**, 1910 (1991).

¹⁰ R. Ballou *et al.*, *J. Magn. Magn. Mater.* **70**, 129 (1987).

¹¹ R. Cywinski, S. H. Kilcoyne, and C. A. Scott, *J. Phys. Condens. Matter* **3**, 6473 (1991).

¹² T. Freltoft *et al.*, *Phys. Rev. B* **37**, 3454 (1988).

¹³ E. Bauer *et al.*, *Int. J. Mod. Phys. B* **7**, 826 (1993).

¹⁴ R. A. Fisher *et al.*, *Int. J. Mod. Phys. B* **7**, 830 (1993).

¹⁵ S. Mondal *et al.*, *Physica B* **180-181**, 108 (1992).

¹⁶ A. Block, M. M. Abd-Elmeguid, and H. Micklitz (unpublished).

¹⁷ J. S. Schilling, U. F. Klein, and W. B. Holzapfel, *Rev. Sci. Instrum.* **45**, 1353 (1974).

¹⁸ R. A. Brand, J. Lauer, and D. M. Herlach, *J. Phys. F* **13**, 675 (1983).

¹⁹ T. Moriya, *Spin Fluctuations in Itinerant Electron Magnetism* (Springer, Berlin, 1985).

²⁰ D. Wagner and E. P. Wohlfarth, *J. Phys. F* **11**, 2417 (1981).

²¹ M. Shiga *et al.*, *J. Phys. Soc. Jpn.* **57**, 1341 (1988).

²² H. Wada, M. Shiga, and Y. Nakamura, *Physica B* **161**, 197 (1989).